

Large format arrays of antenna coupled Kinetic Inductance Detectors for THz astronomy

J. Baselmans^{1,2}, J. Bueno², O. Yurduseven², N. Llombart², S. Yates¹, A. Baryshev^{1,3}, A. Endo^{2,4}, D. Thoen², A. Neto²

¹SRON - Netherlands Institute for Space Research, Sorbonnelaan 2, 3584CA - Utrecht, The Netherlands

²Terahertz Sensing Group, Delft University of Technology, Melkweg 1, 2628CD - Delft, The Netherlands

³Kapteyn Astronomical Institute, University of Groningen, Landleven 12, 9747AD - Groningen, The Netherlands

⁴Kavli Institute of NanoScience, Delft University of Technology, Lorentzweg 1, 2628 CJ Delft, The Netherlands

Abstract—Astronomical observations at infrared, submillimeter, and millimeter wavelengths are essential for addressing many of the key questions in astrophysics. Future ground- and space based observatories need large detector arrays, with more than 10^4 pixels, which are limited only by the noise of the radiation background. We describe in detail a very specific detector, the antenna coupled Microwave Kinetic Inductance Detector and we show that it can provide background limited sensitivity over the entire FIR/mm-wavelength range by choosing different antenna geometries to couple the radiation to the detector. In particular we discuss a narrow band detector coupled to a twin slot antenna at 350 GHz and a broad-band detector coupled to a leaky wave antenna operating from 1.4-2.8 THz. Additionally we demonstrate that we can fabricate, and read-out, large arrays with up to 4000 pixels in a realistic system that can be operated both on ground-based observatories as well as in future space borne observatories

I. INTRODUCTION

Superconducting detectors, operating at extremely low temperatures of 0.1K, are the only detectors capable of reaching the sensitivity requirements for future ground- and space based observatories operating in the infrared, sub-millimeter and millimeter wave wavelengths (0.1 to 30 THz or 3 mm to $10\mu\text{m}$). Several technologies exist, such as bolometers, photoconductors and transition edge sensors, but these technologies present significant fabrication difficulties, and lead to a high degree of complexity of system integration and readout electronics for large format arrays.

The Microwave Kinetic Inductance Detector, or MKID [1], is a relatively new and potentially game-changing superconducting detector technology. It provides background limited sensitivity over the entire FIR/mm-wavelength range and can be adapted for a variety of science goals enabling completely novel instrument concepts. Crucially, they naturally allow to read out in excess of 1000 detectors using a single readout line with very limited cryogenic hardware. In this paper we will describe two different MKID's: A narrow band detector optimised for 350 GHz and a broad band detector operating between 1.4 and 2.8 THz. We will demonstrate that both detectors allow for efficient radiation detection and background limited sensitivity. In the last section we will demonstrate that it is possible to read-out up to 4000 detectors using a single readout chain, consisting of an analog/digital back-end at room

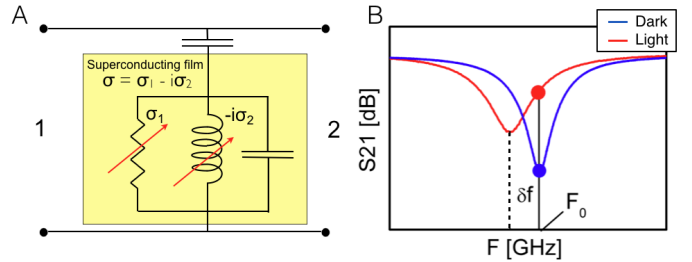


Fig. 1. A) Circuit representation of a single MKID, which is a capacitively coupled resonance circuit with a typical resonance frequency of a few GHz. The measured transmission of such a circuit at low temperature is shown in B) by the 'Dark' curve. Radiation absorption causes the inductance and impedance of the circuit to increase, resulting in a change in the resonance feature depicted by the 'Light' curve. C) The optical NEP measured at a modulation frequency of 200 Hz, NEP_{opt} , as a function of the estimated optical loading, P_{calc} . For every optical loading the NEP in phase (magenta dots) and amplitude (black dots) readout is equal. The measured NEP follows the same slope as $NEP_{calc} \propto \sqrt{P_{calc}}$ (dashed black line). By fitting the relation between the measured NEP and NEP_{calc} (solid black line) an optical efficiency compared to NEP_{calc} is obtained, given by $\epsilon = 1.06 \pm 0.06$. Reproduced from ref.[5].

temperature and 2 coaxial cables connecting the readout to the detector chip.

II. MICROWAVE KINETIC INDUCTANCE DETECTORS

A MKID can be defined as a superconducting film capable of absorbing radiation inside a resonance circuit. This is shown schematically in Fig. 1.A. The superconducting film is represented with a parallel resistance and inductance. The inductance is associated with the Cooper pairs, paired electron states that carry current without any losses. The resistance is associated with electron-like excitations, called quasiparticles, created either by thermal fluctuations or by radiation absorbed in the superconductor. At low temperatures well below the critical temperature of the superconductor (1.2K for aluminium) virtually no quasiparticles exist, resulting in negligible losses. The result is that the circuit will have a very sharp resonance at a frequency of a few GHz as shown in Fig. 1B. Photons with energies larger than the binding energy of a Cooper can be absorbed in the superconducting material by breaking the cooper pairs and creating quasiparticles. This implies that the

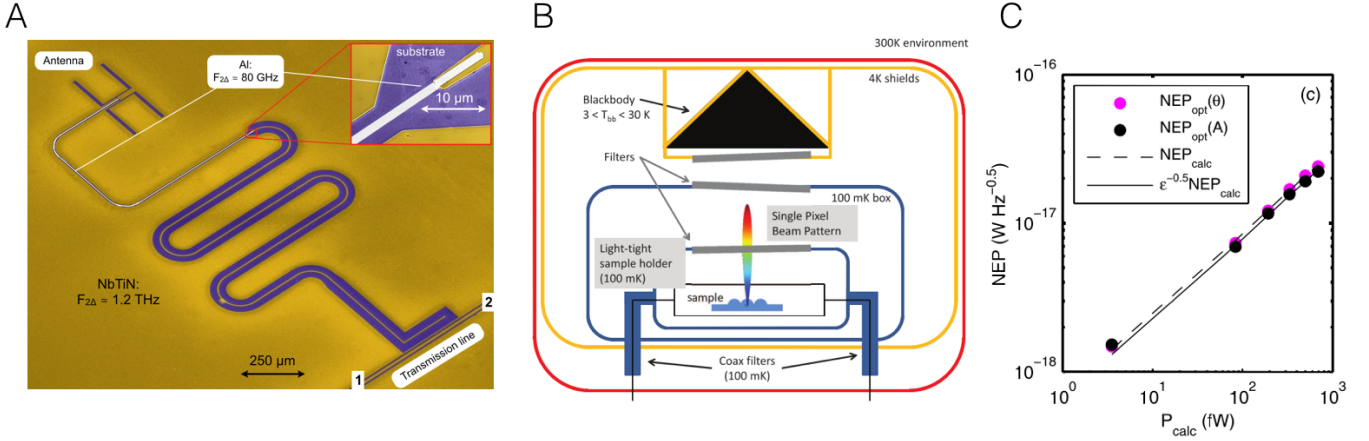


Fig. 2. A) Scanning electron micrograph of the antenna-coupled hybrid NbTiN-Al MKIDs used. A wide NbTiN CPW resonator is used to minimize the two-level system noise contribution. At the shorted end where the planar antenna is located, one millimeter of CPW is reduced in width, and the central line is made from thin Al. The Al is galvanically connected to the NbTiN at both ends (inset) B) Schematic of the setup for measurements at various radiation powers. A blackbody with a variable temperature illuminates the lens antenna-coupled resonators through three stacks of filters, which define a passband around 1.54 THz. Because of the box-in-box configuration at 100mK and the coax cable filters, the device is well shielded from stray light.

frequency of the radiation must exceed the gap frequency $F_{2\Delta}$, which is 80 GHz for aluminium. This process increases the kinetic inductance and the losses in the circuit as indicated by the arrows in the figure. As a result the resonance features shifts to lower frequencies and becomes broader. The MKID is typically read-out using a single frequency readout signal that probes the complex transmission at the unperturbed resonance frequency.

III. TWIN SLOT ANTENNA COUPLED HYBRID MKID AT 350 GHz

In the past years we have developed the hybrid antenna coupled MKID. This device is based upon a distributed, coplanar waveguide (CPW) resonator with a shorted end fabricated on a high dielectric substrate such as silicon or sapphire [5], [6], see Fig. 2. The device is operated at a frequency of around 6 GHz, which corresponds to a 5 mm long resonator operating at its lowest frequency resonance where the device length is 1/4 of the wavelength of the readout signal. The device is fabricated from a 550 nm thick NbTiN film, which has a gap frequency $F_{2\Delta}=1.2$ THz. Below this frequency NbTiN behaves virtually as a perfect conductor. Most of the resonator CPW is relatively wide, with a central line of $5.4\mu\text{m}$ and a gap of $23.7\mu\text{m}$, to reduce intrinsic device noise caused by dielectric fluctuations [3]. The last 1 mm section of the resonator, close to the shorted end, is narrow with a central linewidth = $2.3\mu\text{m}$ and a gapwidth= $3.7\mu\text{m}$. The central line made of Aluminium with a gap frequency of 80 GHz. For the readout signal the material acts as a perfect, lossless conductor, but for any signal with a frequency exceeding 80 GHz the aluminium acts as a normal metal that absorbs radiation: In this process Cooper pairs are broken into quasiparticles resulting in a response from the resonator as described above. To efficiently detect radiation we couple the shorted end of the MKID to a twin slot antenna [2] with a centre frequency of 350 GHz. The

CPW close to the antenna carries 2 signals: The 5 GHz readout signal, which propagates without losses, and the 350 GHz signal from the antenna, which is attenuated by radiation absorption in the aluminium central line. This process requires a distance of 1 mm. The readout signal senses the change in Cooper pair number due to the radiation absorption and the resonance frequency shifts to lower frequencies. The last section of the resonator is narrow because it has: i) to suppress radiation losses at 350 GHz, ii) to increase the responsivity of the device and iii) the shorted end of the resonator does not produce intrinsic noise, as this noise is caused by interactions with the electric field, which is negligible near the shorted end of the resonator [3]. It is worthwhile to mention that this device can be adapted for any frequency between the gap frequency of aluminium (80 GHz) and the gap frequency of NbTiN (1.2 THz) by changing the antenna geometry.

To measure the performance of the detector we mount a small array of 16 detectors, coupled to a monolithic Si lens array of 16 lenses, into a light-tight box at a temperature of 100 mK. The sample holder, and the cold box are closed by infrared filters that transmit radiation only at a ~ 50 GHz band around 350 GHz. Above this assembly we mount a black body radiator whose temperature can be varied between 3 and 40K, which itself is enclosed by a 4K light tight box closed off with another set of filters. The setup schematic is shown in Fig. 2B and explained in more detail in [5], [7]. By measuring the device noise at several temperatures of the radiator together with the response of the detector to a small change in black body temperature we can calculate the noise equivalent power (NEP) of the detector as a function of the radiation power. The result is given in Fig. 2C. The NEP follows a \sqrt{P} dependence, in agreement with background limited performance of the detector. For more details we refer to Ref.[5]. From this data we can directly obtain the total optical efficiency of the

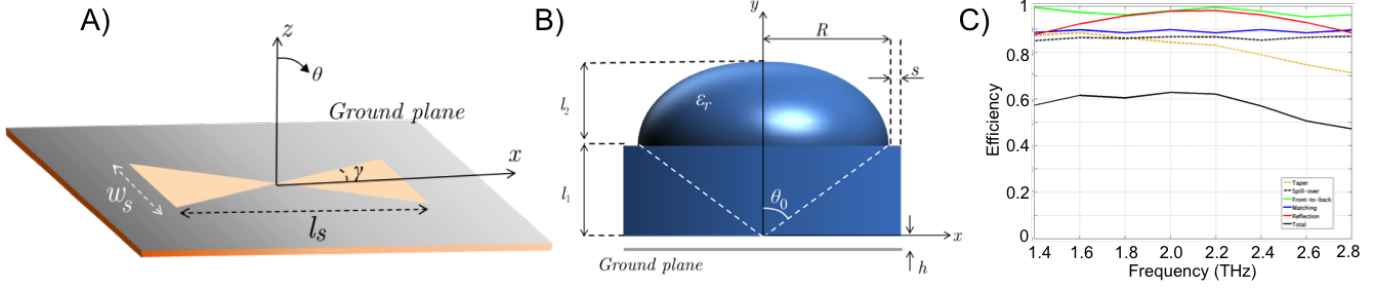


Fig. 3. A) Optimised slot geometry with its design parameters. B) Optimised lens geometry with its design parameters. C) Lens aperture efficiency for the optimised lens coupled leaky wave antenna.

device, which is found to be in excellent agreement with the CST simulation of the lens-antenna system. From this we can conclude that the device has an aperture efficiency of 75%.

IV. LEAKY LENS-ANTENNA COUPLED MKID AT 1.4-2.8 THZ

In this section we will describe a broad band antenna coupled detector where we use a non-resonant planar antennas in order to achieve an octave of bandwidth. We make use of a lens coupled leaky wave antenna in this work because it combines a large bandwidth with a high aperture efficiency. The leaky lens antenna[8] is a lens feed which consists of a leaky-wave slot fabricated on a thin membrane kept at an electrically small distance from the dielectric lens in order to obtain directive radiation inside the lens. This concept has already been proved experimentally[9] at slightly lower frequencies and our current design is based upon these results. The slot width w_s , slot length l_s , slot tapering angle γ and the air-gap between the antenna and the silicon lens h have been optimised to get a more uniform beam at broadside as well as to maximise the difference between the co- and cross-polarisation radiation of the primary fields inside the lens. The optimised design parameters are $w_s=173 \mu\text{m}$, $l_s=602 \mu\text{m}$, $\gamma=15^\circ$ and $h=3 \mu\text{m}$. The geometry of the leaky slot antenna can be seen in Fig. 3.A. The lens is optimised once the dimensions of the single polarisation antenna are set depending on the optimum performance of the primary fields inside semi-infinite dielectric medium. These fields are used assuming that the lens is in the far-field (lens height is about $6\lambda_0$ at the lowest frequency). A parametric study changing the extension length L and the subtended angle θ_0 is done in order to maximise the lens aperture illumination efficiency. The lens schematic can be seen in Fig. 3.B. The optimization process yielded to an extended-hemispherical lens geometry with the following parameters: $l_1=737 \mu\text{m}$, $l_2=442 \mu\text{m}$, $\theta_0=46.5^\circ$, $R=900 \mu\text{m}$, $S=50 \mu\text{m}$, and $L=0.31R$. The efficiency of the optimised antenna can be seen in Fig. 3.C. This efficiency calculation includes the reflection (reflection losses due to the dielectric-air interface on the lens surface) and front-to-back radiation losses (ratio between the power radiated forward and backwards), antenna impedance matching (mismatch between the antenna and feed impedances), spill-over (how much of the

power radiated by the feed is captured by the lens aperture) and taper efficiency (how uniform the effective area of the lens aperture is illuminated). A single matching layer is used in these calculations.

A. Device design and assembly

We have fabricated a 19 pixel array of leaky wave antenna-coupled KIDs, with hexagonal packing and a distance between the pixels of 1.6 mm. The antenna design is optimised for 1.4-2.8 THz radiation detection. This poses a problem in the design, since the gap frequency of NbTiN is 1.2 THz: This material no longer behaves as a perfect conductor as in the 350 GHz case. To solve this problem we use the solution pioneered in Ref. [7]: We use an Al ground plane and an Al central line near the antenna: The field distribution of the THz signal travelling from the antenna is such that 70% of the power is absorbed in the central line where the resulting quasiparticles are confined and thus will be detected. The MKID consists of a wide NbTiN section on the coupler side to reduce the intrinsic device noise (broad strip and gap, 12 and 8 μm respectively) fabricated on a solid Si substrate. The radiation absorbing narrow section and antenna slot are made of Al and fabricated on a free standing 1 μm thick SiN membrane (dimensions of the central line and gap are 0.8 and 1.2 μm respectively). A microscopic picture is shown in Fig. 4.A. Note that the antenna has 2 ports, each connected to a narrow aluminium CPW line line that absorbs the THz radiation. One of these lines is shorted using a NbTiN short, creating both the 1/4 wavelength resonance condition and a quasiparticle diffusion stop. The other line continues as before into the rest of the NbTiN resonator.

The whole detector assembly is made out of three different chips: i) the MKID-antenna chip described above, ii) the spacer wafer that assures a 3 μm gap between the antenna and the lens, and iii) the lens array, as shown in Fig. 4.B. The lens array is made out of a 1 mm thick, high resistivity ($>10 \text{ k}\Omega\text{cm}$) $\langle 100 \rangle$ silicon wafer with a laser ablation technique. The spacer chip is fabricated on a 250 μm thick high resistivity ($>10 \text{ k}\Omega\text{cm}$) $\langle 100 \rangle$ orientation Si wafer covered with a low tensile stress ($\sim 250 \text{ MPa}$) low pressure chemical vapour deposited (LPCVD) silicon nitride (SiN) with a thickness of 300 nm on both sides. A 3 μm gap is etched with reactive

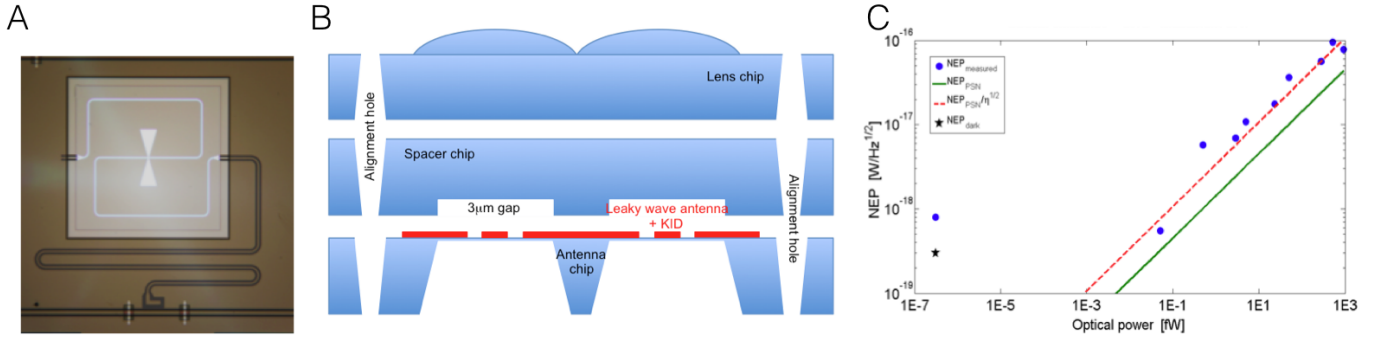


Fig. 4. A) Back and front illuminated optical image of a single pixel. The light goes through the membrane and both the antenna and the part of the MKID on the membrane are illuminated. The rest of the pixel is on the solid substrate. The dark, wide sections are NbTiN, the narrow section is made from Aluminium. B) Schematic drawing of the lens + antenna assembly. The KID and antenna are fabricated on a membrane, a spacer wafer is placed on top of it to assure the 3 μm gap, and the lens goes on top of them. Alignment holes are machined into the three chips and dowel pins are used to assure the alignment accuracy. C) Plot of the optical NEP at a measured frequency of 150 Hz. Blue circles are the measured optical NEP for the phase. The red solid line is the expected photon noise limited NEP and the green dashed line is a fit to the optical NEP to obtain the optical efficiency. The black cross shown the dark NEP for a quasiparticle lifetime of 350 μs , extracted from the noise spectrum at negligible blackbody radiation power.

ion etching (RIE) on the spacer chip at the position where the antennas are placed. A few columns are left on the gap to prevent the membrane of sticking to the spacer chip. The three different chips need to be precisely aligned in order to perform the characterisation of the antenna-coupled KIDs. In order to do the alignment, alignment holes were open in all the wafers. Alignment dowel pins, not shown in the figure, are used to assure the accuracy in the alignment.

B. Experimental results

The experimental procedure is the same as described in Section III, the only difference is that we now use infrared filters that define a 100 GHz band around 1.55 THz. The result is shown in Fig. 4.C. We obtain a minimal optical NEP of 8×10^{-19} W/Hz^{1/2} at very small THz powers. At a THz power exceeding 1 fW we approach a regime where the NEP is background limited and from this regime we can obtain the optical efficiency of the device. From Fig. 3.C) it is clear that we expect a total efficiency of 60% at 1.55 THz when using a matching layer on the lens. In our system, we expect an efficiency of 30%, because of additional reflection losses due to the absence of a matching layer (30% extra losses) and due to the losses of radiation absorption in the ground plane (30% extra losses). Relative to this we measure an efficiency of 65%, i.e. we have 35% unexplained loss of efficiency. Further experiments are being performed to clarify this issue. Both extra losses can be readily eliminated by using a matching layer and by using a thick Al ground plane and a thin Al central line. As shown in [7] *et al.* this reduces absorption in the ground plane to negligible levels. As a cross check we calculate the dark NEP from measurements of the temperature dependence of the KID resonance frequency and Q factor, dark noise, aluminium critical temperature and the quasiparticle lifetime [?]. The dark NEP of the detector is found to be 3×10^{-19} W/Hz^{1/2}, for a quasiparticle lifetime of 350 μs extracted from the roll-off of the noise spectrum

taken at the lowest blackbody power. The ratio between the dark NEP and the optical NEP at negligible loading power is consistent with the measured optical efficiency. Note that the quasiparticle lifetime is short for this device which limits the sensitivity. Normal values of the lifetime in hybrid NbTiN/Al devices are around 1 msec, and also we observe a similar value on aluminium devices on SiN. With such a long quasiparticle lifetime results in a dark NEP of 1×10^{-19} W/Hz^{1/2}. We expect that surface roughening in the fabrication process is responsible for the observed reduction in lifetime. A different fabrication process should be able to eliminate this issue.

V. READOUT

In the previous sections we have shown that antenna coupled NbTiN-Al based hybrid MKIDs can be designed to be background limited detectors at different frequencies and bandwidths. But future observatories do not just need very sensitive detectors, they need very large arrays of these detectors, which requires the development of readout-systems and demonstration of the full system performance. MKIDs are the prime candidate for such large arrays as they are intrinsically easy to multiplex. This is shown in Fig. 5.A. When we design an array of MKIDs make the length of each resonator slightly different (see the inset in panel A). the result is that the resonance frequency of each detector will be slightly different, which makes it possible to have the resonance of about 1000 detectors with in a 2 GHz of bandwidth. In ref. [10] we describe in detail the development of a analog-digital readout system that allows to create up to 4096 readout tones and detect the response of all these tones simultaneously. The central question of such a system is to what extent it degrades the performance of the individual detectors. In Fig. 5.B we show the output noise of a background limited MKID at a loading power of about 0.5 fW, corresponding to a NEP of 1×10^{-18} W/Hz^{1/2}. The two black curves represent the data obtained using a single tone readout system limited only by

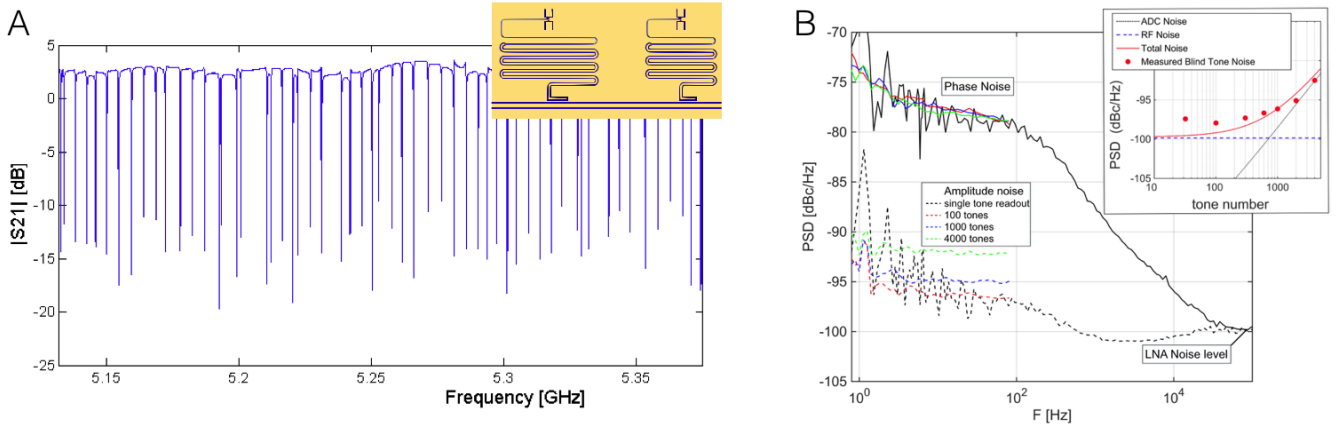


Fig. 5. A) MKID array readout concept. Transmission of a large array of MKIDs. Each resonance feature corresponds to a different MKID. The inset shows 2 MKID detectors with different resonance frequency, set by their length. B) Measured system performance, including RF up- and downconverter on a MKID detecting 1 fW of radiation at 850 GHz, read-out at 4.174 GHz. The black lines represent the phase noise (solid) and amplitude noise (dashed) of the MKID relative to the complex plane measured with a standard single tone homodyne readout. The colored lines represent the performance of the readout presented here. The inset shows the system performance. We refer to the text for details. Reproduced from Ref. [10].

the cryogenic preamplifier at 4K in its readout chain. The solid line represent the noise using phase readout, the dashed line using amplitude readout. For the current discussion we can focus on the solid line that represent phase readout: It represents a readout technique with the same sensitivity but at a much higher output noise level. We plot in colour on the same line the results obtained with the multiplexed readout of Ref.[10], which is reading out 100, 1000 or 4000 tones simultaneously. The inset shows the measured noise performance of this readout as a function of tone number. It is clear that that the device output noise is not affected at all by the multiplexed readout even for 4000 tones. We do clearly see that the bandwidth of the multiplexed readout is limited to 160 Hz, this is however adequate for virtually all applications. This demonstrates that we can read-out very large arrays of MKIDs without degradation of the single pixel performance.

VI. CONCLUSION

We have shown that hybrid NbTiN - Al MKIDs can be used to detect radiation at different frequencies and bandwidths by varying the antenna coupled to the detector. In particular we discuss a 350 GHz, narrow band twin - slot antenna coupled detector and a leaky-wave antenna coupled 1.4-2.8 THz detector. Both devices show background limited performance where the detector sensitivity is only limited by the intrinsic noise of the input signal, i.e. the detector adds no noise of its own to the signal. We also demonstrate that it is possible to read-out up to 4000 of these devices without any reduction in the device sensitivity using a dedicated analog - digital readout system.

ACKNOWLEDGMENT

This work was supported as part of a collaborative project, SPACEKIDS, funded via grant 313320 provided by the Euro-

pean Commission under Theme SPA.2012.2.2-01 of Framework Programme 7.

REFERENCES

- [1] Day P. K., LeDuc H. G., Mazin B. A., Vayonakis A., and Zmudzinas J., 2003, *Nature* 293, 817
- [2] Filipovic D. F., Gearhart S. S., and Rebeiz G. M., 1993, *IEEE Transactions on Microwave Theory and Technology* 41, 1738
- [3] J. Gao, J. Zmudzinas, B. A. Mazin, H. G. Leduc, and P. K. Day, 2007, *Appl. Phys. Lett.*, vol. 90, no. 10, p. 102507
- [4] de Visser P. J., Baselmans J. J. A., Bueno J., Llombart N., and Klapwijk T. M., 2014, *Nature Communications* 5, 3130
- [5] Janssen R. M. J., Baselmans J. J. A., Endo A., Ferrari L., Yates S. J. C., Baryshev A. M., and Klapwijk T. M., 2013, *Applied Physics Letters* 103, 203503
- [6] Yates S. J. C., Baselmans J. J. A., Endo A., Janssen R. M. J., Ferrari L., Diener P., and Baryshev A. M., 2011, *Applied Physics Letters* 99 073505
- [7] de Visser P. J., Baselmans J. J. A., Bueno J., Llombart N., and Klapwijk T. M., 2014, *Nature Communications* 5, 3130
- [8] Neto A., 2010, *IEEE Transactions on Antennas and Propagation* 58, 2238
- [9] Neto A., Llombart N., Baselmans J. J. A., Baryshev A., and Yates S. J. C., 2014, *IEEE Transactions on Terahertz Science and Technology* 4, 26
- [10] J. van Rantwijk, M. Grim, D. van Loon, S. J. C. Yates, A. M. Baryshev and J. J. A. Baselmans, submitted to *IEEE trans on Microwave Theory and Techniques*. See also arXiv:1507.04151 [astro-ph.IM]